

# $^3\text{He}$ in Aerogel – an Inhomogeneously Disordered Unconventional Superfluid

A. Golov, J. V. Porto\*, and J. M. Parpia

Laboratory of Atomic and Solid State Physics,  
Cornell University, Ithaca, New York 14853, USA

*We have examined the superfluidity of  $^3\text{He}$  in 98.2% porous silica aerogel with up to 34%  $^4\text{He}$  at 21.6 bar. The mixture is phase-separated for  $^4\text{He}$  fractions between  $\sim 11\%$  and 34%. The  $^4\text{He}$ -rich phase preferentially occupies the regions of highest silica density in the aerogel, thus modifying the distribution of the correlated disorder seen by superfluid  $^3\text{He}$ . The  $^3\text{He}$   $T_c$  increases slightly with  $^4\text{He}$  content while the superfluid fraction decreases rapidly. This behavior is inconsistent with that of  $^3\text{He}$  in a homogeneously scattering medium and is analogous to that of a granular superconductor.*

*PACS numbers: 67.57.Pq, 64.75.+g.*

## 1. Introduction

Liquid  $^3\text{He}$  is the best understood example of an anisotropically paired superfluid Fermi system. When disordered, this system can lead to new types of ground states as well as provides the means to study how scattering affects the transition temperature,  $T_c$ , and the superfluid component  $\rho_s$ .

In the case of conventional superconductors with paramagnetic impurities, the order parameter can normally be considered as homogeneous though suppressed below its bulk value. In the case of dirty high- $T_c$  superconductors with short coherence lengths, the suppressed order parameter becomes coordinate-dependent, and usually  $\rho_s$  is suppressed more strongly than  $T_c$ .<sup>1</sup> Long-range fluctuations of the density of defects lead to fluctuations of the order parameter. An extreme example of such an inhomogeneity is a gran-

\*Present address: Department of Physics, Massachusetts Institute of Technology, Cambridge, MA 02139, USA

ular superconductor. By weakening the tunneling between the grains it is possible to suppress  $\rho_s$  to zero (at  $T = 0$ ) while  $T_c$  is unchanged and equal to its bulk value.<sup>2</sup>

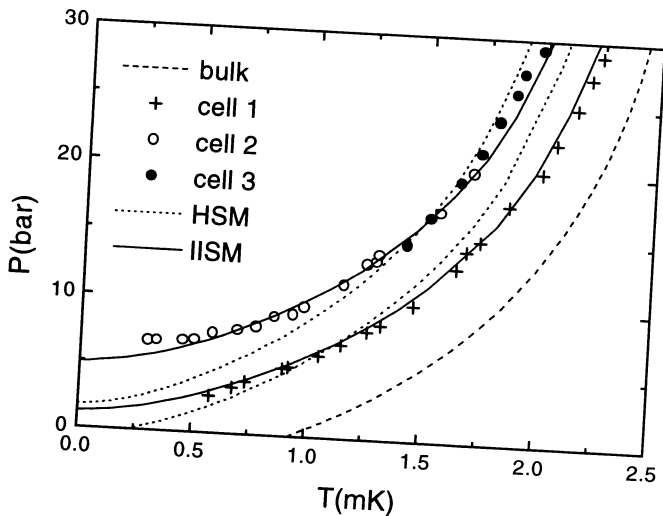


Fig. 1.  $T_c$  vs. pressure in bulk  $^3\text{He}$  (dashed line) and  $^3\text{He}$  in different samples of 98.2% open aerogel (+ - first cell,<sup>3</sup> o - second cell,<sup>5</sup> • - present cell). The calculated (upper/lower) dotted lines correspond to the HSM (mean free path  $l = 1900/2900 \text{ \AA}$ ) and solid lines - to the IISM ( $l = 1900/2900 \text{ \AA}$ , long-range inhomogeneity on the scale  $1300/2000 \text{ \AA}$ ), respectively.

Liquid  $^3\text{He}$  in highly porous aerogel provides a unique opportunity to study the influence of disorder on the triplet superfluid. In 98.2% porous aerogel, the  $^3\text{He}$  superfluid transition is sharp,<sup>3,4</sup> and both  $T_c^{aero}$  and  $\rho_s^{aero}$  were found to be suppressed, although by different amounts dependent on the microscopic structure of the aerogel (Fig. 1). On a microscopic scale the base-catalyzed aerogel is a diffusively aggregated conglomerate of silica particles of  $\sim 50 \text{ \AA}$  size. The disorder, imposed by the aerogel on  $^3\text{He}$ , can be characterized by a broad distribution of correlations in silica (Fig. 2, a, b). For these aerogels of 98.2% porosity, low-angle X-ray scattering<sup>6</sup> revealed that the presence of longer correlations in aerogel results in a smaller  $T_c$  suppression (up to  $\sim 1100 \text{ \AA}$  in the "first cell" (+) and only up to  $\sim 700 \text{ \AA}$  in the "second cell" (o), see Fig. 1). In less open (95%) aerogels no superfluidity has been observed at any pressure,<sup>9</sup> and in more open (99% and 99.5%) aerogels the  $T_c$  and  $\rho_s$  were much less suppressed below bulk values.<sup>10,11</sup>

The internal length scale of  $^3\text{He}$ , the coherence length,  $\xi_0$  (which varies with pressure from  $770$  to  $170 \text{ \AA}$ ), is encompassed by the distribution of

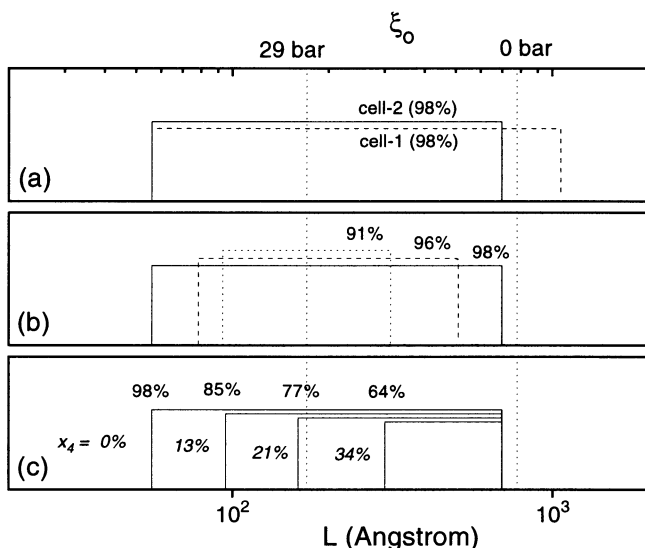


Fig. 2. Cartoon of distributions of length scales for  $^3\text{He}$  in different aerogel samples compared to the coherence length  $\xi_0$  at  $p = 0$  and 29 bar. The vertical scales are for representation only: a) two aerogels (see  $T_c$ 's in Fig. 1) of the same porosity 98.2%, but with different correlations around  $1000 \text{ \AA}$ ;<sup>6</sup> b) three aerogels of different porosities (98%,<sup>6</sup> 96%<sup>7</sup> and 91%<sup>8</sup>); c) our guess of the distributions in a 98% - open aerogel with 0%, 13%, 21% and 34%  $^4\text{He}$  ("effective porosities" 98%, 85%, 77% and 64%).

silica correlations. Initially, it was unclear whether it was important to take long range density fluctuations into account in order to build a theory of  $^3\text{He}$  in aerogel. Neglecting the broad distribution of length scales and accounting for the average silica strand thickness of  $30 \text{ \AA}$ , inter-strand separation of  $200 \text{ \AA}$  and  $^3\text{He}$  quasiparticle mean free path  $l \sim 2000 \text{ \AA}$ , one can expect a nearly homogeneously suppressed order parameter. Thus, the adoption of the Abrikosov-Gor'kov approach<sup>12</sup> should successfully describe the system.<sup>4,13</sup> In such a model both  $T_c^{aero}$  and  $\rho_s^{aero}$  are functions of only  $\xi_0/l$ . A simple test of the model can be performed by deposition of a thick film of  $^4\text{He}$  on the strands, enlarging their average diameter and hence decreasing the  $^3\text{He}$  mean free path  $l$ . One thus should expect suppression of both  $T_c^{aero}$  and  $\rho_s^{aero}$  by the addition of  $^4\text{He}$  to the system.

For pure  $^3\text{He}$  in aerogel, the homogeneous scattering model failed to account for the pressure dependence of  $T_c^{aero}$  and  $\rho_s^{aero}$  (HSM, dotted lines in Fig. 1). Incorporation of the fluctuations of the scattering amplitude on a

single scale  $\sim 1300 - 2000 \text{ \AA}$  (dependent on the aerogel sample) improved the agreement between theory and experiment (isotropic inhomogeneous scattering model, IISM, solid lines in Fig. 1).<sup>13</sup> In order to experimentally determine the role of different length scales of disorder in suppression of the superfluid, we set out to modify the distribution of the correlations relative to  $\xi_0$  and examine how  $T_c^{aero}$  and  $\rho_s^{aero}$  are altered. This was accomplished by coating the aerogel with a thick  $^4\text{He}$  film which preferentially fills the smallest pores and thus raises the lower cut-off of the correlations of disorder sampled by the  $^3\text{He}$  phase (Fig. 2, c). For details see our paper.<sup>14</sup>

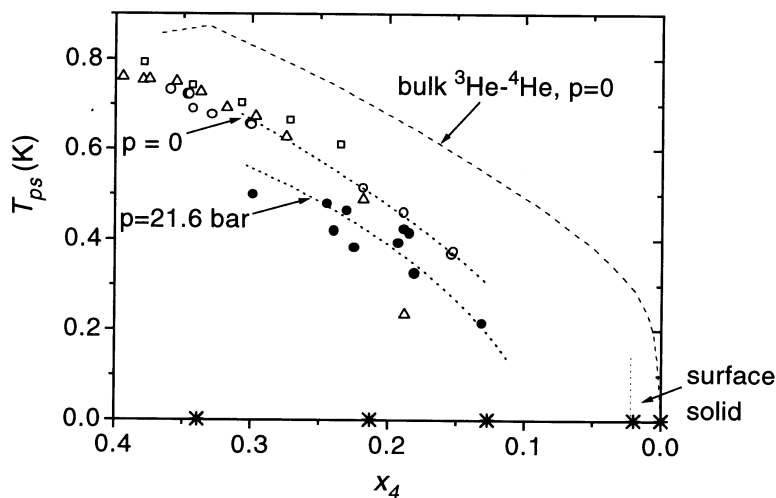


Fig. 3. The temperature of  $^3\text{He} - ^4\text{He}$  phase separation vs.  $^4\text{He}$  concentration in bulk at  $p = 0$  (dashed line) and in 98.2% open aerogel at  $p = 0$  ( $\Delta$  - Kim *et al.*,<sup>15</sup>  $\square$  - Mulders and Chan,<sup>16</sup>  $\circ$  - our data<sup>17</sup>) and at  $p = 21.6$  bar ( $\bullet$  - our data<sup>17</sup>). The dotted lines guide the eye through our data points. The asterisks show  $T_c^{aero} < 2$  mK of five of our samples.

## 2. Technique, Results and Analysis

Aerogel affects the  $^3\text{He} - ^4\text{He}$  phase diagram<sup>15-17</sup> inhibiting phase separation for some range of low  $x_4$  (Fig. 3). In this study we used five  $^4\text{He}$  concentrations  $x_4 = 0, 2.0\%, 12.7\%, 21.3\%$  and  $33.9\%$  at which the mixture is phase-separated at millikelvin temperatures (asterisks in Fig. 3).

We monitored the period,  $P \approx 1.14$  ms, of a torsional oscillator (TO) containing a sample of 98.2% open base-catalyzed aerogel ( $0.4 \text{ cm}^3$  open volume and  $9.3 \text{ m}^2$  area). A concentric-plate capacitor in the head of the TO,

inside which the aerogel was grown (inset to Fig. 4), allows us to determine the molar fraction of  $^4\text{He}$ ,  $x_4$ .<sup>17</sup> The cell also contained a ( $\sim 150 \mu\text{m}$  thick) slab of bulk  $^3\text{He}$  fluid between the aerogel and the mating cup of the TO.

We first surveyed the behavior of pure  $^3\text{He}$  in aerogel as a function of pressure. The  $T_c^{aero}$  ( $\bullet$  in Fig. 1) and  $\rho_s^{aero}/\rho$  as a function of pressure were similar to those of  $^3\text{He}$  in the "second cell"<sup>5</sup> ( $\circ$  in Fig. 1). To examine the effect of  $^4\text{He}$ , we restricted our experimental investigation to a pressure  $p = 21.6 \text{ bar}$  ( $\xi_0 = 200 \text{ \AA}$ ). The period signal for pure  $^3\text{He}$  is shown in Fig. 4.

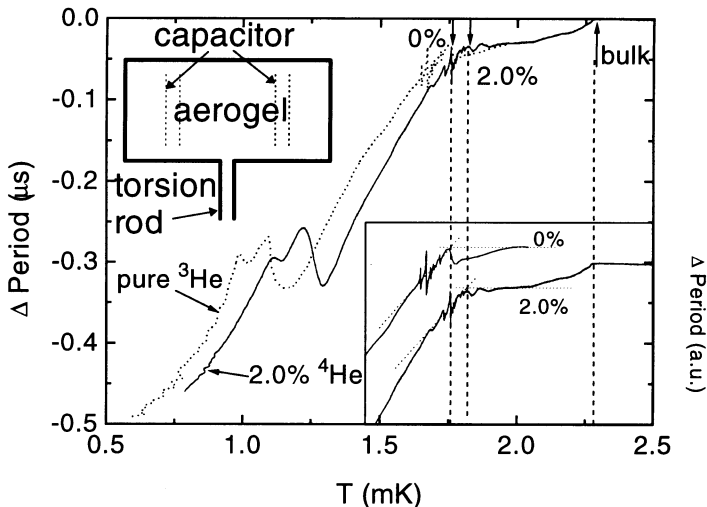


Fig. 4. TO period shifts for pure  $^3\text{He}$  (dotted line) and for 2.0%  $^4\text{He}$  (solid line) at 21.6 bar. Periods have been offset to be identical at  $T_c^{bulk}$ . Vertical dashed lines indicate (from left to right)  $T_c^{aero}$  for pure  $^3\text{He}$ ,  $T_c^{aero}$  for 2.0%  $^4\text{He}$ , and  $T_c^{bulk}$ . The inset in the left shows a schematic of the TO, illustrating the capacitor. The lower inset highlights the region near  $T_c^{aero}$  showing how  $T_c^{aero}$  is determined from the intersection of dotted lines representing  $\Delta P$  vs.  $T$  in aerogel and the behavior in the bulk. The periods are offset for clarity, the temperature scale is identical to that of the main figure.

The cell's construction (the capacitor, large fill line, and an irregular bulk  $^3\text{He}$  volume) results in numerous resonances (Fig. 4), which make the selection of  $T_c$  difficult. With the addition of more than 10%  $^4\text{He}$  these resonances are quenched and replaced with numerous small but reproducible resonances which can give the appearance of noise (Fig. 5).

When 2.0%  $^4\text{He}$  (enough to coat the entire aerogel surface with solid  $^4\text{He}$ ) was added,<sup>18</sup> we observed that  $T_c^{aero}$  increased by  $\sim 0.06 \text{ mK}$  (Fig. 4).

The shift in  $T_c^{aero}$  was determined from the onset of the decrease of the period (Fig. 4, inset). The elevation of  $T_c^{aero}$  by the addition of 2%  $^4\text{He}$  is not directly comparable to that seen by Sprague *et al.*<sup>4</sup> at  $H = 1.5$  kOe. They found the suppression of  $T_c^{aero}$  due to magnetic scattering to be proportional to  $H^2$  and would have predicted no elevation of  $T_c^{aero}$  for  $^4\text{He}$  added at  $H = 0$ .

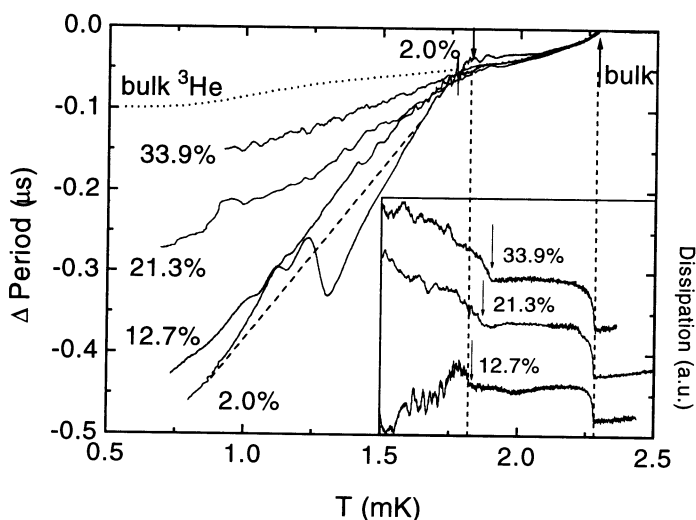


Fig. 5. TO period shifts for four different  $^4\text{He}$  amounts at 21.6 bar. The dotted line shows the contribution from the slab of bulk  $^3\text{He}$ . The dashed line for the 2%  $^4\text{He}$  curve serves to guide the eye through the resonance. Inset: the TO dissipation signal for the 12.7%, 21.3% and 33.9%  $^4\text{He}$  samples showing the sharpness of the transition and how  $T_c^{aero}$  was chosen (arrows). Vertical dashed lines indicate  $T_c^{aero}$  for 2.0%  $^4\text{He}$  (left) and  $T_c^{bulk}$  (right). The temperature scale is identical to that of the main figure.

We then examined samples with 13%, 21% and 34%  $^4\text{He}$  content. Following the addition of  $^4\text{He}$ , we observed a further increase in  $T_c^{aero}$  from 1.82 to 1.90 mK (Fig. 5) while in contrast to the 2%  $^4\text{He}$  results,  $\Delta P$  decreased substantially. With the addition of  $^4\text{He}$ , the strong resonant structure (Fig. 4) is quenched and we were able to use the sharp onset of dissipation (inset to Fig. 5) to fix  $T_c^{aero}$ .

In our analysis we consider the  $^3\text{He}$  -  $^4\text{He}$  mixture to be completely phase separated and the  $^3\text{He}$  and  $^4\text{He}$  superfluids decoupled from each other. The period shift associated with the superfluidity of  $^4\text{He}$  is independent of temperature at  $T < 3$  mK. We also neglect the  $\approx 14\%$  molar volume difference between liquid  $^3\text{He}$  and  $^4\text{He}$ . The  $^3\text{He}$  superfluid component,  $\rho_s^{aero}(T)$ , is

related to the period of the TO,  $P(T)$ , by the relation

$$\frac{\rho_s^{aero}(T)}{\rho} = \frac{1}{1-x_4} \frac{P(T_c) - P(T)}{P_0 - P_{empty}}. \quad (1)$$

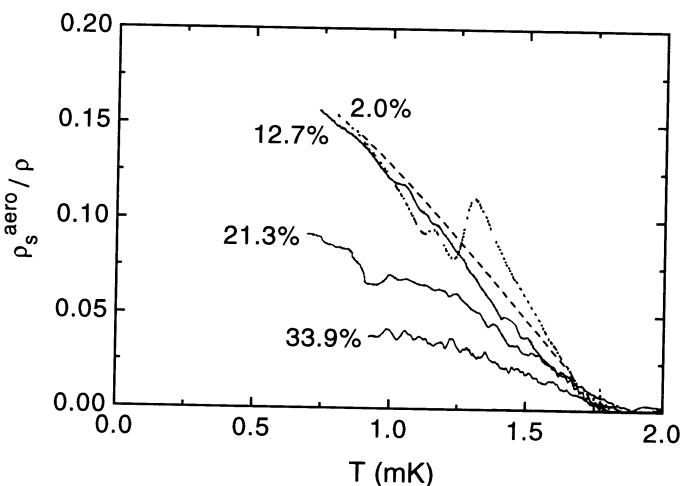


Fig. 6.  $\rho_s^{aero}/\rho$  obtained from the data in Fig. 5 using Eq. 1 after the bulk  $^3\text{He}$  contribution (dotted line in Fig. 5) is subtracted off. The dashed line guides the eye through the resonance in the 2.0%  $^4\text{He}$  data (dotted line).

Here  $P_0 - P_{empty}$  is the total period shift due to filling the cell with pure  $^3\text{He}$  at this pressure and the  $(1-x_4)$  term accounts for the  $^3\text{He}$  volume change due to replacement of  $^3\text{He}$  by  $^4\text{He}$ . From Eq. (1) we can calculate  $\rho_s^{aero}(T, x_4)$ , once the contribution of the bulk  $^3\text{He}$  is subtracted off. We used the known hydrodynamic behavior of bulk  $^3\text{He}$  in a slab<sup>20</sup> (dotted line in Fig. 5) to fit the period shift data in the region between  $T_c^{aero}$  and  $T_c^{bulk}$ . The curves for  $\rho_s^{aero}/\rho$  vs. temperature are shown in Fig. 6. Our results are summarized in Fig. 7 where we show  $\rho_s^{aero}/\rho$  at  $0.5T_c^{aero}$  and  $T_c^{aero}$  for various  $x_4$  in the cell.

### 3. Discussion

When  $x_4$  is increased from zero, a thin film of  $^4\text{He}$  coexists with  $^4\text{He}$  filled pores as a consequence of the interplay between the van der Waals adsorption and capillary condensation. Upon adding  $^4\text{He}$ , successively larger pores are filled with the  $^4\text{He}$ -rich phase, while the remaining surface is still covered with a thin  $^4\text{He}$  film.<sup>21</sup> Eventually, only a thick  $^4\text{He}$ -rich film survives. It

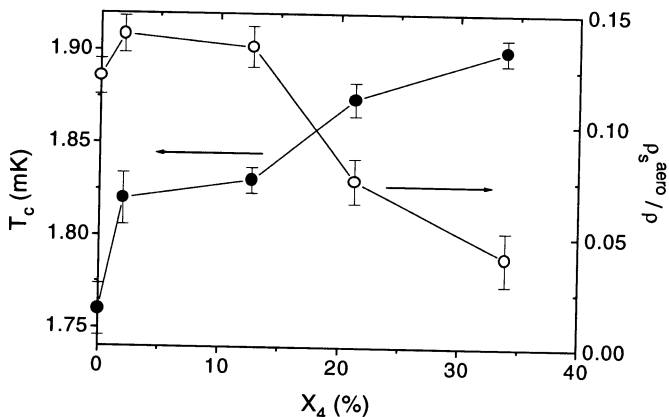


Fig. 7.  $T_c^{aero}$  ( $\bullet$ , left axis) and  $\rho_s^{aero}/\rho$  at  $T = 0.5T_c^{aero}$  ( $\circ$ , right axis) vs.  $x_4$ . The lines connect the data points.

capillary condenses around the regions rich in silica, leaving the  $^3\text{He}$  phase in the center of the open regions devoid of silica (biggest pores), thus altering the structure of the medium sampled by the  $^3\text{He}$  superfluid. At some  $x_4 = x_c \sim 30\%$ , the regions of  $^3\text{He}$  get completely encapsulated by the  $^4\text{He}$ -rich phase and thus isolated into islands. For example, for closely packed identical spherical voids,  $x_c = 1 - \pi/(3\sqrt{2}) = 26\%$ .

The measured  $T_c^{aero}$  and  $\rho_s^{aero}/\rho$  for the sample with 13%  $^4\text{He}$  do not differ much from that with 2%  $^4\text{He}$ , consistent with the system being in the "van der Waals regime". By adding 2% and 13% of  $^4\text{He}$  to  $^3\text{He}$  in 98% porous aerogel we decrease its effective porosity to about 96% and 85%, respectively. The  $^4\text{He}$  occupies the most rough and dense regions of silica leaving the interconnected biggest pores virtually intact.

In the "capillary condensed regime", the connectivity of different parts of  $^3\text{He}$  starts to be affected by  $^4\text{He}$  encapsulation. Hence, the superflow can be suppressed even though the local Cooper pairing is still as strong as it was for pure  $^3\text{He}$ . This picture is consistent with our observation that  $T_c$  is not suppressed further by the addition of  $^4\text{He}$ , but that the  $\rho_s^{aero}$  is (21% and 34% samples). The decrease in  $\rho_s^{aero}$  could be attributed to weakened phase coherence between the more open regions. In this sense, superfluid  $^3\text{He}$  in aerogel with  $\sim 30\%$   $^4\text{He}$  looks similar to a granular superconductor.<sup>2</sup>

The observed enhancement of  $T_c^{aero}$  accompanied by the reduction of  $\rho_s^{aero}$  is inconsistent with the homogeneous scattering model that treats aerogel as a collection of "averaged" strands. A more realistic modification<sup>13</sup> models the long range inhomogeneity of aerogel as a collection of periodi-



cally distributed spherical voids with reduced scattering amplitude. Due to the proximity effect, it produces a single  $T_c^{aero}$  for the sample as a whole. However, the weight of the strongly scattering regions in the determination of  $T_c^{aero}$  is exponentially small compared to that of weak scattering regions. This result is very much in agreement with our finding that  $T_c^{aero}$  slightly increased after the strongly scattering regions are filled with  $^4\text{He}$ . We would conclude that it is misleading to disregard the broad distribution of length scales and to characterize the aerogel by a single averaged parameter (for example, the mean free path).

It is important to note that while  $T_c^{aero}$  of pure  $^3\text{He}$  is very dependent on the porosity of aerogel in the range 99% - 98%, and even on the particular distribution of correlations at the same porosity 98.2%, it virtually isn't altered with the addition of up to 34%  $^4\text{He}$  which effectively decreases the volume available for  $^3\text{He}$  from 98% to 64%. The result is explained in Fig. 2, which illustrates that by changing the aerogel's density or microscopic structure one can affect the long range cut-off of the correlations of the disorder. On the other hand, adding  $^4\text{He}$  affects only the short range side leaving the long range unchanged. It is the presence of long range correlations of the order of  $\xi_0$  which is vital for Cooper pairing and  $T_c^{aero}$ . These correlations can be viewed as an interconnected network of the largest voids, along which most of the superfluid flows.

#### 4. Conclusion

We have examined the superfluid density, transition temperature and  $^4\text{He}$  content of  $^3\text{He}$  -  $^4\text{He}$  mixtures in 98.2% open aerogel using a novel torsion-oscillator and capacitance sensor cell. The results show that the superfluid is very inhomogeneous,  $T_c^{aero}$  is relatively insensitive to the  $^4\text{He}$  content, while  $\rho_s^{aero}$  is suppressed very strongly by the addition of  $^4\text{He}$ .

To summarize, adding  $^4\text{He}$  to  $^3\text{He}$  in aerogel revealed that:

- the "homogeneously scattering medium" approach does not work ( $\rho_s^{aero}$  and  $T_c^{aero}$  change in different directions);
- spatial modulations (long-range inhomogeneity) of the scattering amplitude and order parameter are important;
- the most open regions in aerogel are responsible for the value of  $T_c^{aero}$ , their interconnectivity is responsible for  $\rho_s^{aero}$ ;
- $\sim 34\%$   $^4\text{He}$  is almost enough for encapsulation of the  $^3\text{He}$  in big voids; the phase coherence gets suppressed and so does the long range order;
- decoration of a porous material with a thick  $^4\text{He}$  film is a useful tool to modify the pore size distribution and the interconnectivity of the pores.

## ACKNOWLEDGMENTS

We thank M. H. W. Chan and N. Mulders for the aerogel fabrication. This research was supported under NSF-DMR-9424137.

## REFERENCES

1. M. Franz, C. Kallin, A. J. Berlinsky, and M. I. Salkola, *Phys. Rev. B* **56**, 7882 (1997) and references therein.
2. R. C. Dynes, R. P. Barber, Jr. and F. Sharifi, in *Ordering Disorder: Prospect and Retrospect in Condensed Matter Physics*, edited by V. Srivastava, A. K. Bhatnagar, and D. G. Naugle (AIP, New York, 1993).
3. J. V. Porto and J. M. Parpia, *Phys. Rev. Lett.* **74**, 4667 (1995); *Czech J. Phys.* **46**, 2981 (1996), Suppl. S6.
4. D. T. Sprague, T. M. Haard, J. B. Kycia, M. R. Rand, Y. Lee, P. J. Hamot, and W. P. Halperin, *Phys. Rev. Lett.* **75**, 661 (1995); *ibidem* **77**, 4568 (1996).
5. K. Matsumoto, J. V. Porto, L. Pollack, E. N. Smith, T. L. Ho, and J. M. Parpia, *Phys. Rev. Lett.* **79**, 253 (1997), (E)**79**, 2922 (1997).
6. J. V. Porto *et al.*, to be published.
7. D. W. Schaefer and K. D. Keefer, *Phys. Rev. Lett.* **56**, 2199 (1986).
8. R. Vacher, T. Woignier, J. Pelous, and E. Courtens, *Phys. Rev. B* **37**, 6500 (1988).
9. T. Hall and J. M. Parpia, *Bull. Am. Phys. Soc.* **34**, 1197 (1989).
10. H. Alles, J. J. Kaplinsky, P. S. Wooton, J. D. Reppy, and J. R. Hook, *Physica* (to be published); also in this volume.
11. S. C. J. Kingsley, G. Lawes, A. Golov, K. Matsumoto, J. V. Porto, E. N. Smith, N. Mulders, M. H. W. Chan, and J. M. Parpia, this volume.
12. A. I. Larkin, *JETP Lett.* **2**, 130 (1965).
13. E. V. Thuneberg, S. K. Yip, M. Fogelström, and J. A. Sauls, *Phys. Rev. Lett.* **80**, 2861 (1998).
14. A. Golov, J. V. Porto and J. M. Parpia, *Phys. Rev. Lett.* **80**, 4486 (1998).
15. S. B. Kim, J. Ma, and M. H. W. Chan, *Phys. Rev. Lett.* **71**, 2268 (1993).
16. N. Mulders and M. H. W. Chan, *Phys. Rev. Lett.* **75**, 3705 (1995).
17. A. Golov, J. V. Porto, and J. M. Parpia, *J. Low Temp. Phys.* **110**, 591 (1998).
18. The surface solid has a density of  $\approx 35 \mu\text{mole}/\text{m}^2$  on aerogel.<sup>19</sup> For  $^3\text{He}$  at 21.6 bar this corresponds to about 2.2% of the helium atoms.
19. P. A. Crowell, J. D. Reppy, S. Mukherjee, J. Ma, M. H. W. Chan, D. W. Schaefer, *Phys. Rev. B* **51**, 12721 (1995).
20. J. M. Parpia, D. G. Wildes, J. Saunders, E. K. Zeise, J. D. Reppy, and R. C. Richardson, *J. Low Temp. Phys.* **61**, 337 (1985).
21. P. G. de Gennes, in *Physics of Disordered Materials*, edited by D. Adler, H. Fritzsche, and S. R. Ovshinsky (Plenum, New York, 1985).